Macromolecules

Article

pubs.acs.org/Macromolecules

Water Uptake and Ion Mobility in Cross-Linked Bis(terpyridine)ruthenium-Based Anion Exchange Membranes

Melanie L. Disabb-Miller,[†] Yongping Zha,[‡] Andrew J. DeCarlo,[†] Madhura Pawar,[‡] Gregory N. Tew,*[,‡] and Michael A. Hickner*[,†]

[†]Department of Materials Science and Engineering, The Pennsylvania State University, University Park, Pennsylvania 16802, United States

[‡]Department of Polymer Science and Engineering, University of Massachusetts, Amherst, Massachusetts 01003, United States

Supporting Information

ABSTRACT: As an alternative to benzyltrimethylammonium (BTMA)-functionalized polymers for use as anion exchange membranes (AEMs), we report here on the properties of cross-linked polymers containing tethered bis(terpyridine)ruthenium(II) complexes as AEMs with chloride, bicarbonate, and hydroxide mobile ions. The maximum conductivity for the Ru(II)-complex-based membranes, measured at 30 °C in liquid water, depended on the water uptake and degree of cross-linking more than on the ion exchange capacity (IEC). For membranes with 2:1 cross-linker:monomer ratio, the highest conductivities were 7.9 mS cm^{-1} for the 1.6 mequiv g^{-1} IEC membrane in chloride form, with a hydration number of 51, and 6.5 mS cm^{-1} for the 1.8 mequiv g^{-1} IEC membrane in bicarbonate form, with a hydration number of 124. Additionally, we calculated the chloride and bicarbonate ion diffusion coefficients from conductivity measurements and the samples' hydrated ion concentration, which enabled the membrane ion diffusion coefficients (D) to be related to the dilute solution ion diffusivity (D_0) through the ratio D/D_0. Although membranes with a 1:1 cross-linker:monomer ratio had the lowest barrier to transport, indicated by their high D/D_0 ratio, membranes with a 2:1 cross-linker:monomer ratio demonstrated the highest conductivity due to their balanced water uptake and ion concentration in the hydrated state. At hydration numbers greater than 20, the diffusion coefficient of the mobile chloride or bicarbonate ions was within an order of magnitude of the dilute solution limit. Finally, the properties of the Ru(II)-complex-based AEMs were compared to BTMA-based AEMs by considering the size and charge distribution of the cationic center.

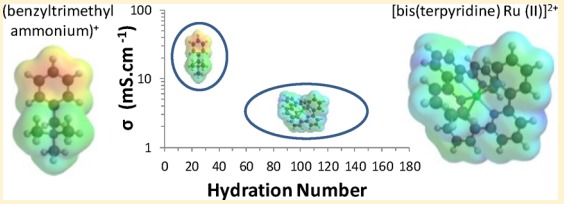

INTRODUCTION

To address ever-increasing global energy demands, means of alternative energy conversion and storage are needed. New materials are being developed that will drive novel energy technologies, including advanced ion-containing polymers as solid electrolytes for fuel cells and electrolyzers.[1,2] A fuel cell membrane must demonstrate high ionic conductivity, good thermal and hydrolytic stability, low fuel crossover, adequate water uptake to facilitate ion conductivity with minimal swelling, low cost, and facile incorporation into membrane electrode assemblies.[3,4] The most popular type of ion-conducting membrane is a proton conducting membrane (PEM) that bears strongly acidic groups to promote water sorption and donate excess protons to solution, which facilitate high proton transport rates through the material. PEM fuel cell and electrolyzer technology requires precious metal catalysts, such as platinum, for high cell performance and catalyst stability in the low pH environment of the acidic membrane. Anion exchange membranes (AEMs) with high internal pH can be constructed largely with non-precious-metal catalysts, but the polymer membrane must remain stable under alkaline conditions and have high anion conductivity, both of which are current challenges in the memberane field.[1−3,5]

Benzyltrimethylammonium (BTMA) and alkyltrimethylammonium cations have been employed in AEMs with poly(arylene ether sulfone),[6,7] poly(fluorenyl ether ketone sulfone),[8] poly(phenylene oxide),[7] poly(tetrafluororoethylene),[9] poly(styrene-*b*-ethylene-*co*-butylene-*b*-styrene),[10] and poly(ether ketone) backbones.[11] Of interest in this effort are a membrane's ion exchange capacity (IEC), conductivity (σ), water uptake (wu), and hydration number (λ), the number of water molecules per (mobile) ion. These quantities must be considered in concert to form a picture of the merits of different approaches to highly anion-conductive membranes. Values for some polymers of interest are shown in Table 1. Examples of AEMs include the work by Guiver and co-workers on BTMA poly(arylene ether sulfone) membranes with an IEC of 1.82 mequiv g^{-1}, hydroxide conductivity at 20 °C of 35 mS cm^{-1}, and λ of 12.3 and on BTMA poly(phenylene oxide) membranes with an IEC of 1.39 mequiv g^{-1}, hydroxide conductivity at 20 °C of 4 mS cm^{-1}, and λ of 10.4.[7] Another series of BTMA poly(arylene ether sulfone) membranes was studied by Yan and Hickner, with IEC ranges

Received: August 13, 2013
Revised: November 6, 2013
Published: November 22, 2013

Table 1. Chemical Structure, Conductivity, and Hydration Number of Several BTMA-Containing Polymers Used as AEMs

Chemical Structure	IEC (meq·g^{-1})	σ (mS·cm^{-1})	λ	Reference
PAES HCO_3^- 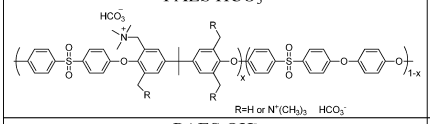	1.48-2.37	6.48-27.3	15-44	Yan and Hickner[6]
PAES OH^- 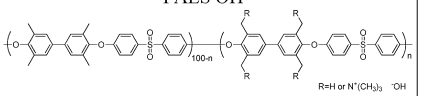	1.82	35	12.3	Li et al.[7]
PPO OH^- 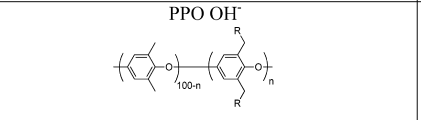	1.39	4	10.4	Li et al.[7]
PPO 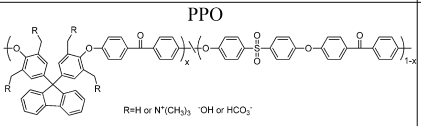	1.8	22.3 (OH^-) 5.1 (HCO_3^-)	18.2 (OH^-) 11.1 (HCO_3^-)	Chen and Hickner[8]
PSEBS OH^- 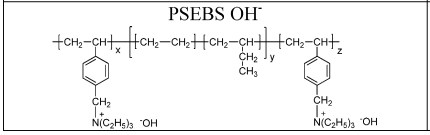	0.578	0.69	5.5	Vinodh, et al.[10]

of 1.48−2.37 mequiv g^{-1}, bicarbonate conductivity at 30 °C ranging from 6.48 to 27.3 mS cm^{-1}, and λ of 15−44.[6] Instead of using a poly(arylene ether sulfone) aromatic backbone, Xiong et al. synthesized a BTMA poly(ether ketone) with an IEC of 0.11 mequiv g^{-1}, hydroxide conductivity of 5.06 mS cm^{-1}, and λ of 16.8.[11] In addition to aromatic backbones, polymers with poly(styrene-*b*-ethylene-*co*-butylene-*b*-styrene)[10] have been used for AEMs; a benzyltriethylammonium poly(styrene-*b*-ethylene-*co*-butylene-*b*-styrene) membrane had an IEC of 0.578 mequiv g^{-1}, hydroxide conductivity of 0.69 mS cm^{-1}, and λ of 5.5.[10] These reports have set the landscape for the possible range of properties of AEMs, but more analysis of the effectiveness of ion conductivity in these examples is warranted.

The decoration of aromatic polymers with BTMA cations is synthetically convenient through chloromethylation of aromatic rings, bromination of benzylic groups, or other halomethylation reactions. However, BTMA, and especially tetraalkylammonium moieties, have well-known degradation mechanisms at high pH that may limit their ultimate stability in AEM applications.[5,12−14] Beyond alkyltrimethylammonium cations, different types of polymer-tethered organic cations such as phosphonium, sulfonium, and imidazolium are being investigated as the fixed charge moiety in AEMs to provide enhanced anion conductivity and stability in these types of polymeric materials. Yan and co-workers have been developing tris(2,4,6-trimethoxyphenyl)benzyl quaternary phosphonium poly(sulfone−methylene) anion exchange membranes with reported hydroxide conductivities of 11, 27, 45, and 38 mS cm^{-1} at 20 °C, depending on the water uptake of the membrane.[15,16] From the reported water uptake values for these materials, we calculated the corresponding λ values to be approximately 24, 33, 53, and 264. Yan and co-workers have also described AEMs consisting of a Udel poly(sulfone) backbone functionalized with triarylsulfonium groups. The hydroxide conductivity of the sulfonium-containing poly(sulfone) with an IEC of 0.68 mmol g^{-1} was 7.7 mS cm^{-1} at 20 °C (λ or water uptake were not reported). However, the hydroxide conductivity of a similar IEC sample (0.69 mmol g^{-1}) more than doubled to 15.4 mS cm^{-1} at 20 °C for a calculated λ of 22 when the poly(sulfone) was functionalized with diphenyl(3-methyl-4-methoxyphenyl) tertiary sulfonium cations.[17]

Although imidazolium-functionalized AEMs have been investigated as a more stable alternative to materials with BTMA cations, imidazolium ionic groups have not been clearly demonstrated to have enhanced properties compared to BTMA-containing membranes. A 1-methyl benzylimidazolium-functionalized poly(fluorenyl ether ketone sulfone) membrane with an IEC of 1.64 mequiv g^{-1} demonstrated bicarbonate conductivity of 3.9 and hydroxide conductivity of 17.1 mS cm^{-1} for λ values of 9.9 and 14.8, respectively. In the same study, this membrane was directly compared to a BTMA-functionalized poly(fluorenyl ether ketone sulfone), which exhibited higher conductivity and water uptake with bicarbonate conductivity of 5.1 mS cm^{-1} and hydroxide conductivity of 22.3 mS cm^{-1} for λ values of 11.1 and 18.2, respectively.[8] This report demonstrated the usefulness of BTMA cations compared to N-linked 1-methylimidazolium cations generated from simple synthetic methods. 1,2-Dimethyl-3-alkylimidazolium functional groups were also used by Lin et al. in conjunction with poly(fluorene) to produce an AEM with an IEC of 0.98 mequiv g^{-1}. The hydroxide conductivity was 23.5 mS cm^{-1} at 30 °C, with a calculated λ of 10, which was about twice that of the bicarbonate conductivity of the same membrane. The conductivity was comparable to that of a similar BTMA-functionalized polymer.[18]

In addition to considering different ionic groups for AEM functionalization, another strategy for achieving next-generation AEMs is to cross-link polymers to minimize membrane swelling, even at high IEC. Pan et al. observed only 3%

dx.doi.org/10.1021/ma401701n | Macromolecules 2013, 46, 9279−9287

swelling at 80 °C for their BTMA poly(sulfone) polymers that were cross-linked by exposing the chloromethylated polymer to stoichiometric quantities of diethylamine, producing tertiary benzyldiethylamino groups on the polymer backbone. The residual benzyl chloride moieties were then further reacted with trimethylamine, resulting in a poly(sulfone) with both tertiary amino groups and BTMA groups. Subsequently, any remaining chloromethyl groups reacted with the tertiary amino groups on the polymer backbone to form cross-links during the membrane casting process.[19] Self-cross-linking quaternary phosphonium tris(2,4,6-trimethoxyphenyl) poly(sulfone−methylene) membranes resulting from the reaction of benzylchloromethyl groups and trimethyoxyl benzene rings possessed 5−10 times lower swelling ratio than non-cross-linked membranes with the same IEC.[20] The cross-linking was performed at 80 °C without a catalyst, allowing for a one-pot process. For quaternary phosphonium functionalized membranes with IEC values of approximately 1.0, 1.17, and 1.23 mequiv g^{-1} at 60 °C, the cross-linked membranes had calculated λ values of 9 (17 wt % wu), 16 (33 wt % wu), and 45 (99 wt % wu), respectively, while the non-cross-linked membranes had much higher calculated λ values of 40 (71 wt % wu), 120 (254 wt % wu), and 1114 (2469 wt % wu), respectively. The hydroxide conductivity was 38 mS cm^{-1} at 20 °C for the 1.23 mequiv g^{-1} cross-linked membrane (λ = 45), which was consistent with the conductivity of the non-cross-linked membrane in both quaternary phosphonium and BTMA forms.[20]

Another method of producing cross-linked AEMs was developed by Coates and co-workers, who employed ring-opening metathesis polymerization (ROMP) of a tetraalkylammonium-functionalized norbornene with dicyclopentadiene (DCPD). The resulting cross-linked fully hydrated membrane (λ or water uptake were not reported) demonstrated hydroxide conductivities at 20 °C of 14 and 18 mS cm^{-1} for samples with 2:1 DCPD:monomer (1.0 mequiv g^{-1} IEC) and 1:1 DCPD:monomer (1.4 mequiv g^{-1} IEC) ratios, respectively.[21] Also synthesized using ROMP, a phosphonium-functionalized poly(ethylene) with an IEC of 0.67 mequiv g^{-1} was found to have hydroxide conductivity of 22 mS cm^{-1} and λ of 43.[22]

Recently, we introduced bis(terpyridine)Ru(II)-based AEMs, which were the first metal-cation containing AEMs, using the ROMP technique with DCPD cross-linking moieties described above. The use of the metal Ru(II) complex in an AEM was targeted toward increased anion conductivity by allowing for two counterions to be involved in ion transport, instead of the single counterion typically associated with tethered cations such as BTMA. The conductivity and hydration values of these membranes were highly dependent on the degree of cross-linking present in the membranes. The hydroxide conductivity at 30 °C ranged from 14 to 28 mS cm^{-1}, for membranes with IEC values of 1.0−2.0 mequiv g^{-1} and λ values of 30−216, depending on the DCPD:heteroleptic bis(terpyridine)Ru(II) complex ratio in the membrane.[23] Taking into account the high water uptake of the bis(terpyridine)Ru(II)-based AEMs, the conductivity values of the membranes were at the lower end of the range reported in the literature. A larger series of Ru (II)-based AEMs was developed in an effort to improve conductivity while decreasing membrane swelling.

At this point, the key strategies for improved AEM performance are unclear, but by studying the relationships between fixed ion concentration, water diffusion, morphology, and ion conductivity, promising directions in the field can be identified. The goal of this work is to report optimized compositions and properties for bis(terpyridine)Ru(II)-based AEMs and compare their intrinsic ion conduction performance to more commonly explored BTMA-based AEMs.

EXPERIMENTAL METHODS

Polymer Synthesis and Membrane Preparation. The heteroleptic bis(terpyridine)Ru(II) complex-functionalized norbornene monomer was synthesized according to our previous report.[23] In order to maintain the same cross-linking density while varying the IEC, a hydrophobic comonomer, 1,5-cyclooctadiene (COD), was introduced to the system. COD is inexpensive and highly soluble in the same solvent mixture as the other two components. Its complete polymerization by Grubbs' second generation catalyst (G2) only takes about 10 min at room temperature.[24] The Ru(II) complex cationic monomer, COD, and DCPD were dissolved together in a chloroform/methanol solvent mixture at room temperature. After adding G2 and stirring vigorously for 1 min, the homogeneous solution was transferred to a flat, preheated aluminum pan where the polymerization continued at 40 °C for ∼1 h. A translucent, ∼100 μm-thick membrane in chloride form was obtained following solvent evaporation. Subsequent ion exchange in sodium bicarbonate solution yielded the AEM samples in the bicarbonate form. For further information regarding the membrane purification, refer to the Supporting Information.

Characterization. Conductivity measurements were performed using impedance spectroscopy on a Solartron 1260A impedance/gain-phase analyzer. The impedance of free-standing films was measured using a two-point, in-plane geometry at frequencies between 1 MHz and 100 Hz.[25] During the measurements, humidity and temperature were controlled with an ESPEC SH-241 environmental chamber. The relative humidity (RH) was controlled from 20% to 95% while the temperature was held at 30 °C. The real value of the impedance, where the imaginary response was zero, was used as the membrane resistance and the ion conductivity (σ) was calculated from

$$\sigma = \frac{L}{RA} \tag{1}$$

where L is the length between electrodes, R is the resistance of the membrane, and A is the cross-sectional area of the membrane. In general, the conductivity measurements presented in this work have errors of ±20%.

The activation energy for ion conduction, E_a, was calculated from conductivity measurements with the sample immersed in liquid water between 30 and 70 °C (in 10 °C steps). The logarithm of conductivity versus $1/T$ was linearly regressed and the Arrhenius activation energy was computed from the slope of the best fit regression line.

Bicarbonate conductivities were measured by exchanging the chloride form membranes in 1 M sodium bicarbonate at room temperature for 24 h followed by extensive rinsing to remove excess salt. Hydroxide conductivities were measured by exchanging the bicarbonate form membranes in 1 M KOH solution for 8−12 h. The membranes were then rinsed with degassed, 18.2 MΩ·cm water to remove excess ions and placed into conductivity cells and immersed in liquid water that was degassed and blanketed with flowing Ar. The impedance was measured over a period of 3 h under Ar, and then the Ar blanket was removed and the conductivity was measured over a number of days with the water exposed to ambient conditions containing the natural amount of CO_2, ∼395 ppm (Figure S5).

Water uptake (wu = $(m_{hyd} - m_0)/m_0$), where m_{hyd} is the hydrated sample mass and m_0 is the dry sample mass, was measured as a function of relative humidity using a TA Instruments Q5000SA water vapor sorption microbalance at 30 °C between relative humidities of 20% and 95%. The hydration number (λ), or the number of water molecules per ionic group, was calculated from

$$\lambda = \left(\frac{m_{hyd} - m_0}{m_0}\right)\left(\frac{1000}{M_{H_2O}\mathrm{IEC}}\right) \tag{2}$$

dx.doi.org/10.1021/ma401701n | Macromolecules 2013, 46, 9279−9287

Scheme 1. Monomers Polymerized by Grubbs Second Generation Catalyst into Resulting Chemical Structure Overlayed on Optical Image of a Membrane

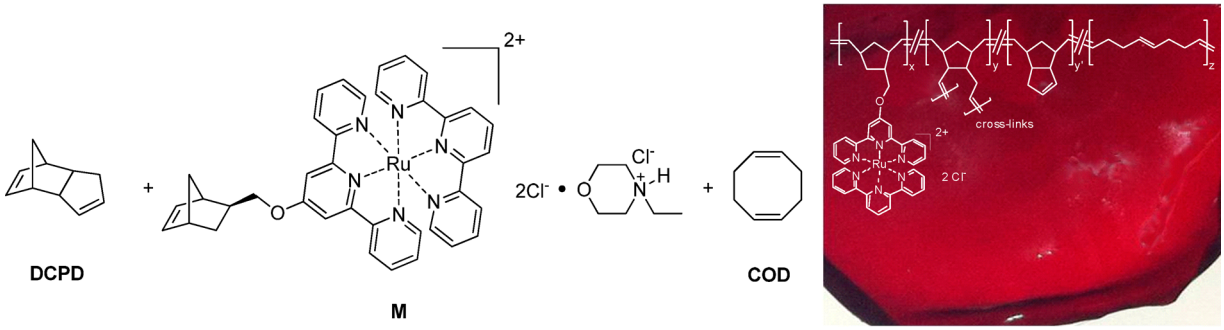

Table 2. Membrane Sample Parameters and Properties[a]

[DCPD]:[M+COD]	[M]:[COD]	IEC (mequiv g^{-1})	wu_{Cl^-} (mass %)	λ_{Cl^-}	σ_{Cl^-} (mS cm^{-1})	$wu_{HCO_3^-}$ (mass %)	$\lambda_{HCO_3^-}$	$\sigma_{HCO_3^-}$ (mS cm^{-1})	σ_{OH^-} (mS cm^{-1})	$E_{a\_Cl^-}$ (kJ mol^{-1})	$E_{a\_HCO_3^-}$ (kJ mol^{-1})
1:1	3:7	1.4	197	78	5.3	398	158	3.5	8.9	6.4	11.4
1:1	4:6	1.6	417	145	3.5	461	160	4.7	nm	5.5	6.8
2:1	3:7	1.0	38	21	6.1	117	65	3.0	10.0	19.9	17.7
2:1	5:5	1.4	103	41	5.9	133	53	5.5	13.0	5.9	13.5
2:1	6:4	1.6	148	51	7.9	260	90	2.7	10.6	9.9	18.3
2:1	8:2	1.8	246	85	6.8	358	124	6.5	15.2	14.3	11.2
5:1	6:4	1.0	24	13	3.6	39	21	2.4	4.0	15.6	25.9

[a]Water uptake (wu), hydration number (λ), conductivity (σ), and activation energy (E_a) are reported for fully hydrated membranes. Measurements that were not obtained are denoted by nm.

where m_{hyd} is the hydrated sample mass, m_0 is the mass of the dry sample, M_{H_2O} is the molecular mass of water (18.02 g mol^{-1}), and IEC is the ion exchange capacity with units of milliequivalents of ions per gram of polymer.

For liquid water uptake measurements, the fully hydrated anion exchange membranes were removed from liquid water, blotted quickly to remove surface water, and weighed immediately. The measurement was repeated 3−5 times after soaking the membrane in liquid water to rehydrate the membrane and obtain an accurate hydrated sample mass. The membranes were then dried at 80 °C in vacuum for 48 h and at 120 °C in vacuum for 48 h (96 h total) and weighed again to obtain m_0.

The mechanical properties of the membranes in the bicarbonate form were characterized using an Instron 4468 load frame equipped with a 50 N static load cell at a constant crosshead speed of 5 mm min^{-1}. Samples were cut into a dog bone shape with a gauge length of 16 mm and width of 5 mm. Measurements were performed at room temperature on samples immediately removed from water after being immersed for at least 24 h to ensure complete hydration.

The molecular modeling software Spartan version 4.0.1 from Wave function, Inc., was used for cation size and surface potential calculations and assumed the molecule was in a vacuum. The electron density surface calculations used the Hartree−Fock calculation model and the 3-21G(*) split-valence basis set. The semiempirical Pm3(tm) model was used for mapping the electrostatic potential on the electron density surface, since parametrizations for transition metals are available in this model. The electron density mapping gave the overall size, shape, and position of the chemical bonds in the molecule. The electrostatic potential was mapped, giving both steric and electrostatic characteristics of the molecule by the variation in color representing electron-rich and electron-poor regions. The common scale in Spartan visualization was set to 43 to 152 (red to blue), with the colors at the red end of the spectrum representing the electron-rich regions and those at the blue end representing electron-poor regions.

RESULTS AND DISCUSSION

The synthesis scheme for these heteroleptic bis(terpyridine)-Ru(II) complex-based AEMs with COD and DCPD cross-linking is shown in Scheme 1. Briefly, the bis(terpyridine)Ru-(II) complex monomer (M) was combined with COD and DCPD at room temperature to form the membranes. The ratio of M to COD determined the IEC of the membranes. As in our previous work, the Ru monomer was isolated as a cosalt,[23] and extensive soaking after formation of the membrane was used to remove the *N*-ethylmorpholinium chloride from the cross-linked membranes, which was confirmed by FTIR analysis (Figure S1). Stability of these AEMs in an alkaline environment was investigated by UV−vis spectroscopy, using the three representative absorption peaks for the Ru complex in the UV−vis region (Figure S2) as well as measuring the change in mass with time (Figure S3). The UV−vis measurements did not show significant shifts in the absorption peaks, and the mass change measurements showed no significant mass loss or degradation of the membranes in alkaline conditions (1 M NaOH) at elevated temperatures (80 °C). Compared to the AEMs consisting of only the Ru monomer and DCPD,[23] addition of COD into the system did not seem to have any significant impact on the alkaline stability of the membranes. The water uptake, conductivity at 30 °C, and activation energy of the membranes studied are listed in Table 2.

Membranes in bicarbonate form demonstrated higher water uptake and hydration numbers than the corresponding membranes in their chloride form. The highest conductivity values were obtained for membranes in hydroxide form, which we partly attribute to the greater dilute solution mobility of hydroxide ions, 197.6 × 10^{-5} cm^2 V^{-1} s^{-1}, compared to the dilute solution mobilities of bicarbonate and chloride ions, 46.4 × 10^{-5} and 76.3 × 10^{-5} cm^2 V^{-1} s^{-1}, respectively.[26,27]

dx.doi.org/10.1021/ma401701n | *Macromolecules* 2013, 46, 9279−9287

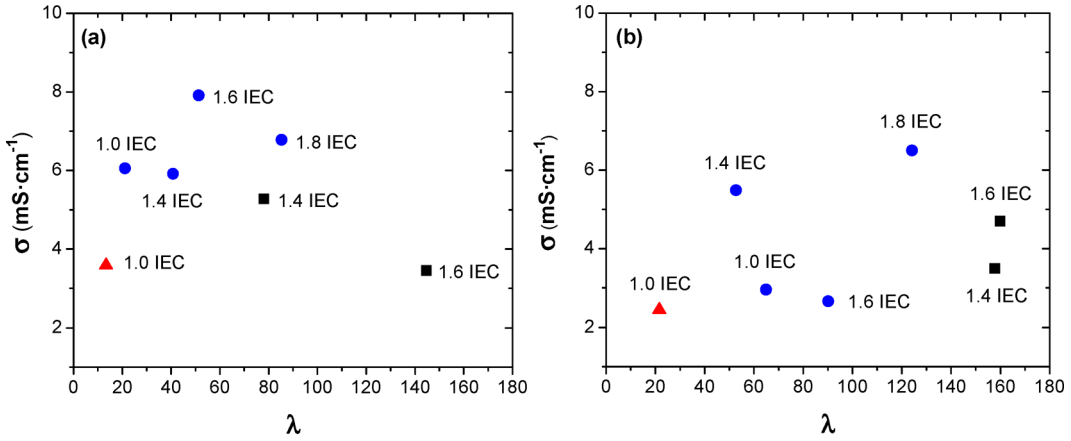

Figure 1. Conductivity of membranes as a function of hydration number in the (a) chloride form and (b) bicarbonate form for (■) [DCPD]:[M + COD] = 1:1, (blue ●) [DCPD]:[M+COD] = 2:1, and (red ▲) [DCPD]:[M + COD] = 5:1. The maximum conductivity occurred at a hydration number of approximately 50 and 125 for membranes in chloride form and bicarbonate form, respectively.

For the membranes in the chloride form, the maximum conductivity occurred at a λ value of 51, as shown in Figure 1. The cross-linking ratio was critical to both conductivity and water uptake, with 2:1 [DCPD]:[M + COD] yielding the highest conductivity sample. For membranes with the same IEC, the 2:1 [DCPD]:[M + COD] membrane demonstrated higher conductivity and lower water uptake compared to the 1:1 [DCPD]:[M + COD] membrane. We believe the membranes in hydroxide form absorbed more water than the other anion forms due to the thermodynamic driving forces involved with hydration. The Gibbs free energy of hydration for hydroxide ions is −430 kJ mol^{-1}, compared to −335 kJ mol^{-1} for bicarbonate ions and −340 kJ mol^{-1} for chloride ions.[28] When the membranes were converted to bicarbonate form, the 1.8 mequiv g^{-1} IEC sample had the highest conductivity of 6.5 mS cm^{-1} at λ = 124. Such high values for hydration number at maximum conductivity are in stark contrast to PEMs of the perfluorosulfonic acid variety, with maximum conductivity at $\lambda \sim 22$.[29]

To further study the effect of cross-linking on water uptake and conductivity of the Ru-based AEMs, we calculated the ion concentration for the membranes from the volume-based water uptake using

$$c = 0.001\frac{\rho(\mathrm{IEC})}{1 + 0.01X_{\mathrm{v-H_2O}}} \quad (3)$$

where c is the moles of ions per cm^3 of polymer, ρ is the polymer density, IEC is the milliequivalents of ion per gram polymer, and $X_{\mathrm{v\text{-}H_2O}}$ is the volume-based water uptake.[30] As illustrated by Figure 2, the membranes with the highest conductivity in the chloride form had between approximately 5 × 10^{-4} and 7.5 × 10^{-4} mol of Cl$^-$ per cm^3 of polymer. The maximum conductivity was observed for the sample with 6.5 × 10^{-4} mol cm^{-3}, and there was clear differentiation between the conductivity values of the samples with a [DCPD]:[M + COD] ratio of 2:1 and those with different cross-linker ratios.

The mechanical properties of the membranes in the bicarbonate form are shown in Table 3. The tensile modulus of the membrane samples increased with the degree of cross-linking and decreased with increasing hydration. The tensile stress at break followed the same behavior, but the tensile strain at break decreased with the degree of cross-linking and increased with greater membrane hydration. This data suggests

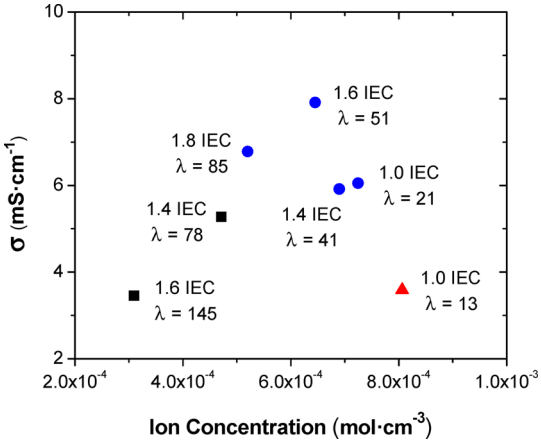

Figure 2. Role of ion concentration on membrane conductivity for membranes in the chloride form with [DCPD]:[M + COD] ratios of (■) 1:1, (blue ●) 2:1, and (red ▲) 5:1. The IEC and hydration number of the membranes are denoted next to the corresponding symbols.

that for better mechanical performance of the membranes there is an optimal cross-link density and IEC that must be obtained. Although the membranes exhibited excessive swelling, the tensile stress and strain at break of the 5:1 [DCPD]:[M + COD] membrane were comparable to the values reported by Coates and co-workers for their tetraalkylammonium-functionalized norbornene and DCPD membranes with 2.3 ± 0.5 MPa tensile stress at break and 26 ± 3% tensile strain at break.[21]

The hydration numbers of the membranes in the chloride form were inversely related to the ion concentration (Figure 3). Higher IEC membranes on a gravimetric basis swelled more with liquid water than low IEC membranes, and the ion concentration in the hydrated material was lower for the high IEC samples. This swelling behavior, leading to dilution of the fixed charge groups, was dictated by the cross-linking ratio of the material, where the more highly cross-linked samples showed lower water uptakes. For low cross-linking ratios, the samples swelled significantly, even at low IEC. It appears from the data in Figure 3 that an intermediate level of cross-linking was required in these samples to balance the water uptake and ion concentration to obtain high conductivity.

dx.doi.org/10.1021/ma401701n | Macromolecules 2013, 46, 9279−9287

Table 3. Mechanical Properties of the Membranes in Bicarbonate Counterion Form[a]

[DCPD]:[M+COD]	IEC (mequiv g^{-1})	$wu_{HCO_3^-}$ (mass %)	$\lambda_{HCO_3^-}$	tensile modulus (MPa)	tensile stress at break (MPa)	tensile strain at break (%)
1:1	1.4	398	158	0.017 ± 0.003	0.17 ± 0.03	50 ± 14
2:1	1.0	117	65	0.083 ± 0.014	0.75 ± 0.20	33 ± 2
2:1	1.4	133	53	0.023 ± 0.003	0.50 ± 0.01	71 ± 4
5:1	1.0	39	21	0.50 ± 0.06	1.9 ± 0.2	21 ± 1

[a]The membranes with IEC = 1.6 and 1.8 mequiv g^{-1} were too brittle to test.

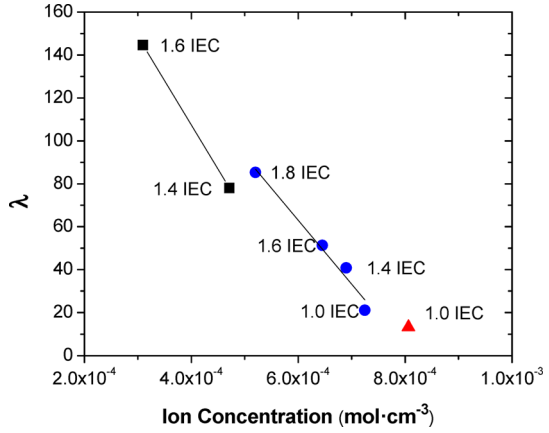

Figure 3. Hydration number decreased as ion concentration increases for membranes in chloride form with [DCPD]:[M + COD] ratios of (■) 1:1, (blue ●) 2:1, and (red ▲) 5:1.

To compare conductivity values of membranes with different IECs, a few studies have reported an IEC-normalized conductivity, which is calculated by dividing the measured conductivity by the membrane IEC.[20,31,32] However, this analysis approach does not account for differences in ion mobility, which is important when comparing membranes with different mobile ion species. As discussed previously, the dilute solution mobility of hydroxide ions, 197.6 × 10^{-5} cm^2 V^{-1} s^{-1}, is higher than the dilute solution mobilities of bicarbonate and chloride ions, 46.4 × 10^{-5} and 76.3 × 10^{-5} cm^2 V^{-1} s^{-1}, respectively.[26,27] To address the difference in mobility for different conductive species, mobility-normalized conductivity, where the measured conductivity is divided by the mobility of the conductive ion, has also been used to investigate membrane transport properties and compare PEMs and AEMs.[33] This approach is still limited for ion transport analysis and does not incorporate the water-swollen membrane ion concentration. A more rigorous method for analyzing conductivity of these materials employs the information obtained from conductivity and water uptake of the polymer membranes to calculate the effective diffusion coefficients (D) of the mobile ions in PEMs and AEMs. For the Ru(II)-complex-based AEMs, the effective diffusion coefficients of the mobile ions were calculated from a form of the Nernst−Einstein equation:

$$D = \frac{\sigma RT}{cz^2F^2} \tag{4}$$

where σ is the measured conductivity, R is the ideal gas constant, T is temperature, c is the computed concentration of ions in mol/cm^3 calculated by eq 3, z is valence charge, and F is Faraday's constant.[34] For each ion, we determined the barrier to ion transport by comparison of the calculated effective ion diffusion coefficients to the ion diffusivity in dilute solution (D_0), the maximum diffusivity of an ion in water.[35] The dilute ion diffusivity is calculated from the dilute solution mobilities of the mobile ion using

$$D_0 = \frac{\mu k_B T}{q} \tag{5}$$

where μ is the dilute solution ion mobility, k_B is the Boltzmann constant, T is temperature, and q is the ion charge.[36] The ratio of the diffusion coefficient to the dilute ion diffusivity (D/D_0), shown in Figure 4, should approach a value of unity, or the dilute solution limit, at high water uptake where the sample is composed largely of water.[34,36] However, although the D/D_0 ratio increased with increasing hydration for membranes in the chloride and bicarbonate forms, the highest D/D_0 ratios obtained were 0.17 at λ = 85 for the 1.8 mequiv g^{-1} IEC, 2:1

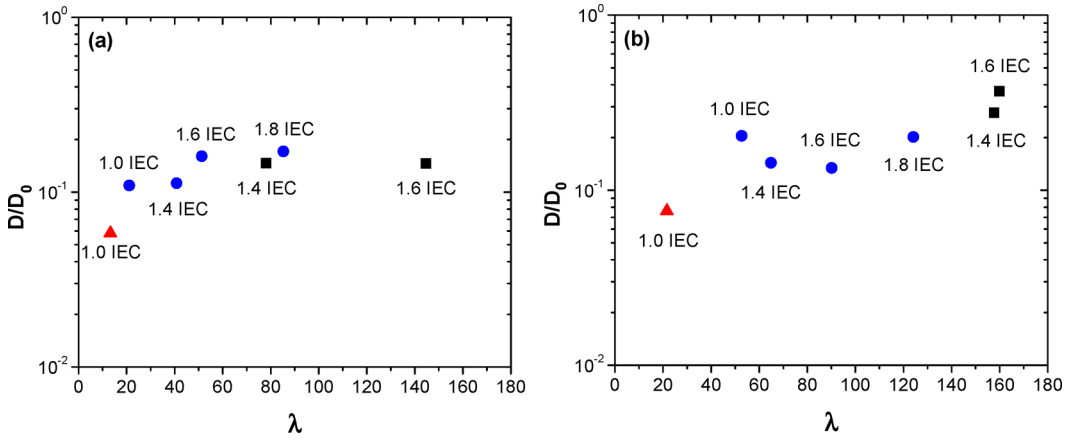

Figure 4. Ratio of the effective diffusion coefficient, D, to the dilute solution diffusivity, D_0, as a function of hydration number for membranes in the (a) chloride form and (b) bicarbonate form, with [DCPD]:[M + COD] ratios of (■) 1:1, (blue ●) 2:1, and (red ▲) 5:1. The higher D/D_0 ratio for the bicarbonate ions signifies that the bicarbonate diffusion coefficient in the samples was closer to the dilute solution diffusivity of bicarbonate ions.

dx.doi.org/10.1021/ma401701n | Macromolecules 2013, 46, 9279−9287

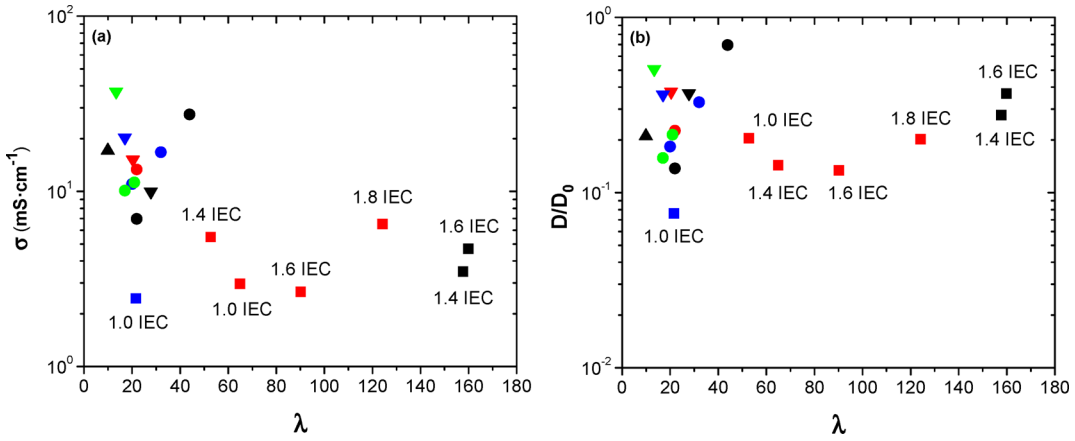

Figure 5. Ion transport properties of membranes in the bicarbonate form, for Ru (II) complex-based membranes with [DCPD]:[M+COD] ratios of (■) 1:1, (red ■) 2:1, and (blue ■) 5:1; BTMA-based tetramethylbisphenol membranes with (●) 100, (blue ●) 80, (red ●) 60, and (green ●) 40 mol % tetramethylbisphenol;[6] (▲) imidazolium-based poly(fluorenyl ether ketone sulfone) membrane;[8] and phosphonium-based bromomethylated poly(2,6-dimethyl-1,4-phenylene oxide) membranes with (▼) 20%, (blue ▼) 34%, (red ▼) 57%, and (green ▼) 90% degree of functionalization,[38] where (a) depicts bicarbonate conductivity as a function of hydration number and (b) illustrates the ratio of the effective diffusion coefficient, D, to the dilute solution diffusivity, D_0, as a function of hydration number.

[DCPD]:[M + COD] membrane in the chloride form and 0.37 at λ = 160 for the 1.6 mequiv g^{-1} IEC, 1:1 [DCPD]:[M + COD] membrane in the bicarbonate form. Despite the fact that bicarbonate anions have lower dilute solution mobilities than chloride anions, we observed that samples in the bicarbonate form had higher effective ion diffusivities compared to their dilute solution limit due to their greater hydration numbers. The larger water uptake led to decreased ion concentration and higher diffusion coefficients for the membranes in the bicarbonate form. The overall higher hydration number of bicarbonate forms, compared to chloride, despite similar free energies of hydration, could be a result of processing to exchange the ions from chloride (as made) to bicarbonate, which can cause irreversible swelling and thus increases the water uptake of the bicarbonate form samples. Additionally, based on the Hofmeister effect, bicarbonate ions are more kosmotropic than chloride ions, meaning they are more highly hydrated and thus may draw more water into the sample upon ion exchange.[37]

To compare the behavior of the bis(terpyridine)Ru(II) complex-based AEMs with other common functional groups used in AEMs, we show in Figure 5 the bicarbonate conductivity and D/D_0 ratio with respect to hydration for several membranes from the literature (values are in Table S1). Compared to BTMA, benzyl-1-methylimidazolium, and benzyl tri(methoxyphenyl)phosphonium-based membranes, the bis-(terpyridine)Ru(II) membranes demonstrated lower bicarbonate conductivity and greater hydration numbers. Despite the decreased bicarbonate conductivity, the D/D_0 for the metal-complex membranes for cross-linking ratios of 2:1 and 1:1 is similar to the BTMA-based samples.

We hypothesize that the differences in volume and charge density between the BTMA cation and the bis(terpyridine)-Ru(II) cationic complex are responsible for the differences in hydration and ion diffusion within the materials discussed above. Shown in Figure 6 are the calculated volumes for the BTMA (187 Å^3) and bis(terpyridine)Ru(II) cations (496 Å^3). The volumetric charge density for each species is 187 and 248 Å^3/charge, respectively. The lower charge density of the bis(terpyridine)Ru(II) cation likely promoted weaker localized hydration around the cationic center. Water is dispersed around

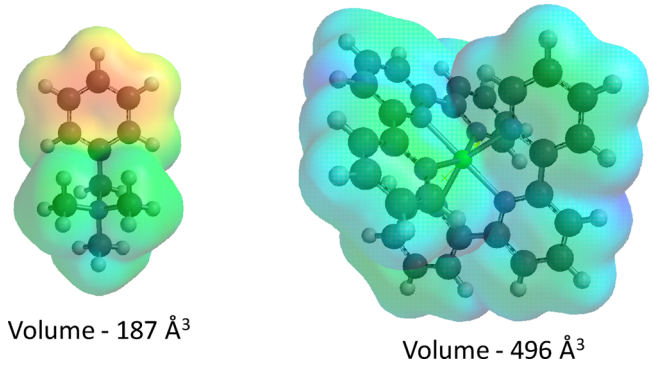

Figure 6. Molecular volume calculated from Spartan for (left) BTMA and (right) bis(terpyridine)Ru(II) cations.

the complex leading to high hydration of the material without drastically increasing the ion conductivity. The electrostatic surface potential maps in Figure 7 show that there is still significant electron deficiency in the terpyridine rings, and the charge deficiency of the terpyridine ligands is similar to the

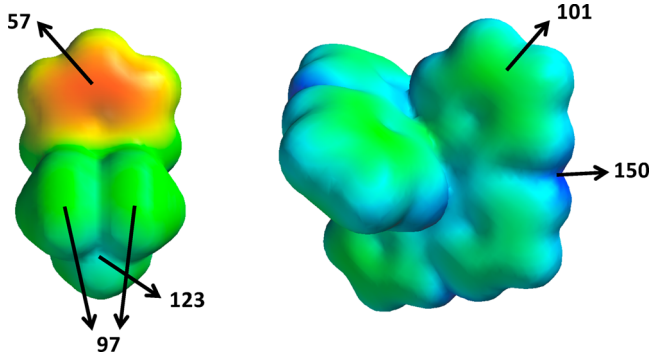

Figure 7. Electrostatic potential map with orange, and green colors depicting more electron-rich regions and blue depicting more electron-poor regions for (left) BTMA and (right) bis(terpyridine)Ru(II) cations. Common scale in Spartan visualization was set to 43 to 152 (red to blue). Arrows depict regions with specific electrostatic potentials.

dx.doi.org/10.1021/ma401701n | Macromolecules 2013, 46, 9279−9287

trimethylammonium center. Water can localize in the electron-poor region of the BTMA cation, promoting ion motion and connectivity of watery domains for effective ion conduction. Conversely, based on the charge density calculations, water can be distributed around the bis(terpyridine)Ru(II) cation, so greater hydration is required for fast ion transport. These differences in hydration led to the lower bicarbonate conductivity and higher hydration numbers for the metal-complex AEMs compared to BTMA, quaternary phosphonium, and imidazolium-functionalized AEMs, as previously shown in Figure 5. While explicit water calculations are beyond the scope of the present study, the effects of water clustering in anion exchange membranes on conductivity as promoted by cation and backbone type are a fertile and important area for future mechanistic studies.

CONCLUSIONS

The conductivity and hydration of bis(terpyridine)Ru(II) complex-based membranes are dominated by the cross-linking ratio, [DCPD]:[M + COD]. The IEC played a minor role in the properties of these materials, but it appeared that a balance between sufficient water uptake and ion concentration was critical to promote good conductivity. The maximum conductivity of these membranes in chloride form (σ_{Cl^-} = 7.9 mS cm^{-1}) was observed at a hydration number of 50, which is greater than other AEMs and sulfonated polymers. At high water uptake, the ions in the Ru(II) complex-based membranes did not reach the dilute solution diffusivity limit of the mobile species, indicating the presence of barriers to transport, even in highly hydrated materials. The large size of the bis(terpyridine)-Ru(II) cation, combined with its uniform electrostatic surface potential, led to greater hydration requirements for adequate ion motion. Continued work on these membranes will focus on increasing the mechanical strength of the polymers while maintaining their conductivity and reducing swelling. In addition, understanding the role of the metal within the cation will be essential, and these studies are underway.

ASSOCIATED CONTENT

Supporting Information

Detailed characterization data of the polymer and membranes, including FTIR spectra of byproduct removal; UV−vis spectra and mass loss data regarding membrane stability; effective diffusion coefficient and dilute solution diffusivity values for the membranes as well as graphs illustrating the conductivity ratios of the ions, decay of the hydroxide conductivity with time, and hydration of the membranes as a function of RH. This material is available free of charge via the Internet at http://pubs.acs.org.

AUTHOR INFORMATION

Corresponding Authors

*E-mail hickner@matse.psu.edu (M.A.H.).
*E-mail tew@mail.pse.umass.edu (G.N.T.).

Notes

The authors declare no competing financial interest.

ACKNOWLEDGMENTS

This work was supported in part by the National Science Foundation (CBET-0932740), ARO (W911NF-09-1-0373), and ONR (N00014-10-1-0348). We are also grateful for the support of the Materials Research Science and Engineering Center (MRSEC) at the University of Massachusetts Amherst (DMR-0820506). Mass spectral data were obtained at the University of Massachusetts Mass Spectrometry Facility, which is supported, in part, by the National Science Foundation.

REFERENCES

(1) Hickner, M. A. *Mater. Today* **2010**, *13*, 34−41.
(2) Couture, G.; Alaaeddine, A.; Boschet, F.; Ameduri, B. *Prog. Polym. Sci.* **2011**, *36*, 1521−1557.
(3) Merle, G.; Wessling, M.; Nijmeijer, K. *J. Membr. Sci.* **2011**, *377*, 1−35.
(4) Deabate, S.; Gebel, G.; Huguet, P.; Morin, A.; Pourcelly, G. *Energy Environ. Sci.* **2012**, *5*, 8824−8847.
(5) Varcoe, J. R.; Slade, R. C. T. *Fuel Cells* **2005**, *5*, 187−200.
(6) Yan, J.; Hickner, M. A. *Macromolecules* **2010**, *43*, 2349−2356.
(7) Li, N.; Zhang, Q.; Wang, C.; Lee, Y. M.; Guiver, M. D. *Macromolecules* **2012**, *45*, 2411−2419.
(8) Chen, D.; Hickner, M. A. *ACS Appl. Mater. Interfaces* **2012**, *4*, 5775−5781.
(9) Salerno, H. L. S.; Elabd, Y. A. *J. Appl. Polym. Sci.* **2013**, *127*, 298−307.
(10) Vinodh, R.; Ilakkiya, A.; Elamathi, S.; Sangeetha, D. *Mater. Sci. Eng., B* **2010**, *167*, 43−50.
(11) Xiong, Y.; Liu, Q. L.; Zeng, Q. H. *J. Power Sources* **2009**, *193*, 541−546.
(12) Komkova, E.; Stamatialis, D.; Strathmann, H.; Wessling, M. *J. Membr. Sci.* **2004**, *244*, 25−34.
(13) Edson, J. B.; Macomber, C. S.; Pivovar, B. S.; Boncella, J. M. *J. Membr. Sci.* **2012**, *399−400*, 49−59.
(14) Chempath, S.; Boncella, J. M.; Pratt, L. R.; Henson, N.; Pivovar, B. S. *J. Phys. Chem. C* **2010**, *114*, 11977−11983.
(15) Gu, S.; Cai, R.; Luo, T.; Chen, Z.; Sun, M.; Liu, Y.; He, G.; Yan, Y. *Angew. Chem., Int. Ed.* **2009**, *48*, 6499−6502.
(16) Gu, S.; Cai, R.; Luo, T.; Jensen, K.; Contreras, C.; Yan, Y. *ChemSusChem* **2010**, *3*, 555−558.
(17) Zhang, B.; Gu, S.; Wang, J.; Liu, Y.; Herring, A. M.; Yan, Y. *RSC Adv.* **2012**, *2*, 12683−12685.
(18) Lin, B.; Qiu, L.; Qiu, B.; Peng, Y.; Yan, F. *Macromolecules* **2011**, *44*, 9642−9649.
(19) Pan, J.; Chen, C.; Zhuang, L.; Lu, J. *Acc. Chem. Res.* **2012**, *45*, 473−481.
(20) Gu, S.; Cai, R.; Yan, Y. *Chem. Commun.* **2011**, *47*, 2856−2858.
(21) Clark, T. J.; Robertson, N. J.; Kostalik, H. A.; Lobkovsky, E. B.; Mutolo, P. F.; Abruña, H. D.; Coates, G. W. *J. Am. Chem. Soc.* **2009**, *131*, 12888−12889.
(22) Noonan, K. J. T.; Hugar, K. M.; Kostalik, H. A.; Lobkovsky, E. B.; Abruña, H. D.; Coates, G. W. *J. Am. Chem. Soc.* **2012**, *134*, 18161−18164.
(23) Zha, Y.; Disabb-Miller, M. L.; Johnson, Z. D.; Hickner, M. A.; Tew, G. N. *J. Am. Chem. Soc.* **2012**, *134*, 4493−4496.
(24) Bielawski, C. W.; Grubbs, R. H. *Angew. Chem., Int. Ed.* **2000**, *39*, 2903−2906.
(25) Fujimoto, C. H.; Hickner, M. A.; Cornelius, C. J.; Loy, D. A. *Macromolecules* **2005**, *38*, 5010−5016.
(26) Voet, D.; Voet, J. G. *Biochemistry*, 4th ed.; John Wiley & Sons: New York, 2011; p 45.
(27) Vanysek, P. In *CRC Handbook of Chemistry and Physics*; Lide, D. R., Ed.; CRC Press: Boca Raton, FL, 2002.
(28) Marcus, Y. *Biophys. Chem.* **1994**, *51*, 111−127.
(29) Suarez, S. N.; Jayakody, J. R. P.; Greenbaum, S. G.; Zawodzinski, T.; Fontanella, J. J. *J. Phys. Chem. B* **2010**, *114*, 8941−8947.
(30) Kim, Y.; Einsla, B.; Sankir, M.; Harrison, W.; Pivovar, B. *Polymer* **2006**, *47*, 4026−4035.
(31) Grew, K. N.; Chu, D.; Chiu, W. K. S. *J. Electrochem. Soc.* **2010**, *157*, B1024.
(32) Zhang, B.; Gu, S.; Wang, J.; Liu, Y.; Herring, A. M.; Yan, Y. *RSC Adv.* **2012**, *2*, 12683.
(33) Hibbs, M. R.; Hickner, M. A.; Alam, T. M.; Mcintyre, S. K.; Fujimoto, C. H.; Cornelius, C. J. *Chem. Mater.* **2008**, *20*, 2566−2573.

(34) Walls, H. J.; Fedkiw, P. S.; Zawodzinski, T. A.; Khan, S. A. *J. Electrochem. Soc.* **2003**, *150*, E165−E174.
(35) Disabb-Miller, M. L.; Johnson, Z. D.; Hickner, M. A. *Macromolcules* **2013**, *46*, 949−956.
(36) Muthukumar, M.; Rice, S. A. *Adv. Chem. Phys.* **2005**, *131*, 45.
(37) Liu, L.; Wang, T.; Liu, C.; Lin, K.; Ding, Y.; Liu, G.; Zhang, G. *J. Phys. Chem. B* **2013**, *117*, 2535−2544.
(38) Jiang, L.; Lin, X.; Ran, J.; Li, C.; Wu, L.; Xu, T. *Chin. J. Chem.* **2012**, *30*, 2241−2246.